

# PIXELHOP++: A SMALL SUCCESSIVE-SUBSPACE-LEARNING-BASED (SSL-BASED) MODEL FOR IMAGE CLASSIFICATION

Yueru Chen\*, Mozhdeh Rouhsedaghat\*, Suya You<sup>+</sup>, Raghuveer Rao<sup>+</sup> and C.-C. Jay Kuo\*

\* University of Southern California, Los Angeles, California, USA

<sup>+</sup> Army Research Laboratory, Adelphi, Maryland, USA

## ABSTRACT

The successive subspace learning (SSL) principle was developed and used to design an interpretable learning model, known as the PixelHop method, for image classification in our prior work. Here, we propose an improved PixelHop method and call it PixelHop++. First, to make the PixelHop model size smaller, we decouple a joint spatial-spectral input tensor to multiple spatial tensors (one for each spectral component) under the spatial-spectral separability assumption and perform the Saab transform in a channel-wise manner, called the channel-wise (c/w) Saab transform. Second, by performing this operation from one hop to another successively, we construct a channel-decomposed feature tree whose leaf nodes contain features of one dimension (1D). Third, these 1D features are ranked according to their cross-entropy values, which allows us to select a subset of discriminant features for image classification. In PixelHop++, one can control the learning model size of fine-granularity, offering a flexible tradeoff between the model size and the classification performance. We demonstrate the flexibility of PixelHop++ on MNIST, Fashion MNIST, and CIFAR-10 three datasets.

**Index Terms**— Small learning models, interpretable learning models, successive subspace learning, image classification.

## 1. INTRODUCTION

The design of small machine learning models is a hot research topic in recent years since small models are essential to mobile and edge computing applications. There has been a lot of research dedicated to neural network model compression and acceleration, *e.g.* [1, 2, 3, 4, 5]. Techniques such as parameter pruning, quantization, binarization and sharing, low-rank factorization, transferred filters, knowledge distillation, etc. have been applied to larger network models to achieve this goal. Another path is to design small network models from the scratch. Examples include SqueezeNet [6], SquishedNets [7] and SqueezeNet-DSC [8]. Being similar to the situation with large neural-network-based learning models, the underlying mechanism of small learning models remains to be a mystery.

Being inspired by study on deep learning networks, the successive subspace learning (SSL) principle was recently proposed. It has been used to design two interpretable machine learning models – PixelHop for image classification [9] and PointHop for point cloud classification [10]. Since no backpropagation is needed in SSL-based model training, the training can be done efficiently. In this work<sup>1</sup>, we focus on the model size (in terms of model parameters)

of PixelHop and propose several ideas to reduce its model size, resulting in a new method called PixelHop++.

This work has several contributions. First, we point out the weak correlation of different spectral components of the Saab transform, which is used in PixelHop for dimension reduction. Then, we exploit this property to design a channel-wise (c/w) Saab transform, which can reduce the filter size as well as the memory requirement for filter computation in PixelHop++. Second, we propose a novel tree-decomposed feature representation method whose leaf node provides a scalar (or 1D) feature. By concatenating leaf node's features, we obtain a feature vector of higher dimension for PixelHop++. Third, we compute the cross-entropy value of each feature and order them from the lowest to highest. The feature of lower cross-entropy has higher discriminant power. As a result, we can find a proper subset of features that are suitable for the classification task. In PixelHop++, one can control the learning model size of fine-granularity, offering a flexible tradeoff between the model size and the classification performance. We demonstrate the flexibility of PixelHop++ on MNIST, Fashion MNIST, and CIFAR-10 three datasets.

## 2. BACKGROUND REVIEW

Subspace learning is one of the fundamental problems in signal/image processing and computer vision [11, 12, 13, 14, 15, 16]. The subspace method learns a projection from an input data space into a lower-dimensional subspace which serves as an approximation to the input space. Being inspired by the deep learning (DL) framework and built upon the foundation in [17, 18, 19, 20], Kuo *et al.* proposed the successive subspace learning (SSL) principle to design interpretable machine learning models. Concrete examples include PixelHop [9] and PointHop [10], which are designed for image and point cloud classification problems, respectively. Their model parameters are determined stage-by-stage in a feedforward manner without any backpropagation (BP).

The PixelHop method contains three main modules: 1) successive near-to-far neighborhood expansion and unsupervised dimension reduction; 2) supervised dimension reduction via designed label-assisted regression (LAG); 3) feature concatenation and decision making. PixelHop extracts features successively from a pixel and its near-, mid- and far-range neighborhoods in multiple stages, where each stage corresponds to one PixelHop unit. To control the rapid growth of the output dimension of a PixelHop unit, the Saab (subspace approximation with adjusted bias) transform [20] is

policies, either expressed or implied, of the U.S. Army Research Laboratory or the U.S. Government. The U.S. Governments are authorized to reproduce and distribute reprints for Government purposes notwithstanding any copyright notation hereon.

<sup>1</sup>This research was supported by the U.S. Army Research Laboratory's External Collaboration Initiative (ECI) of the Director's Research Initiative (DRIA) program. The views and conclusions contained in this document are those of the authors and should not be interpreted as representing the official

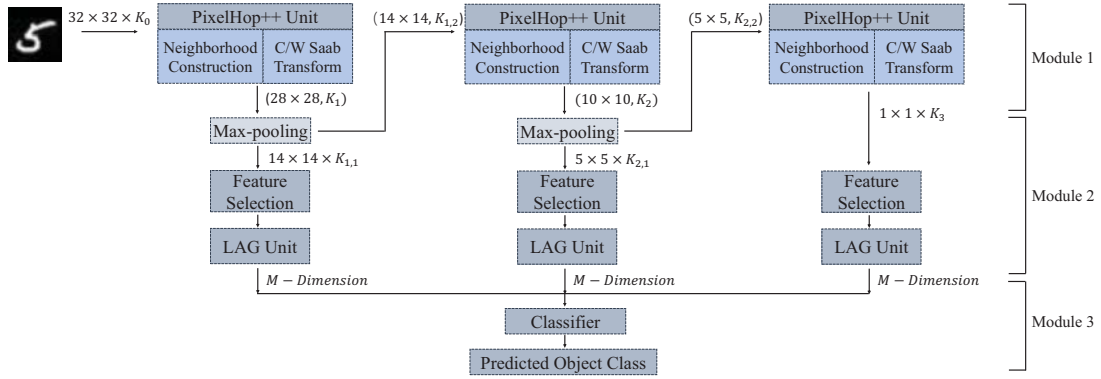


**Fig. 1:** The block diagram of the PixelHop++ method that contains three PixelHop++ Units in cascade.

adopted for unsupervised dimension reduction.

### 3. PROPOSED PIXELHOP++ METHOD

The block diagram of the PixelHop++ method for tiny images (size  $32 \times 32$ ) is shown in Fig. 1. It has three PixelHop++ units in cascade. In all of them, the Saab transform kernels are of the same spatial dimension ( $5 \times 5$ ). Also, We apply the max pooling operation to filtered outputs in the first and the second PixelHop units. As compared with PixelHop, PixelHop++ has the following three modifications.

1. We replace the traditional Saab transform with the channel-wise (c/w) Saab transform.
2. A novel tree-decomposed feature representation is constructed.
3. We order leaf node's features based on their cross-entropy values and use them to select a feature subset.

They will be detailed below.

#### 3.1. Channel-wise (c/w) Saab Transform

Module 1 in Fig. 1 is an unsupervised feature learning module. By arguing that the Saab transform can be approximated by the tensor product of two separable transforms - one along the spatial domain and the other along the spectral domain, we can reduce the size of the Saab transform. The Saab transform is a variant of the PCA (Principal Component Analysis) transform. Since PCA can decorrelate the covariance matrix into a diagonal matrix, all channel components are decoupled. Although the Saab transform is not identical with the PCA transform, we expect Saab coefficients to be weakly correlated in the spectral domain.

To validate the spatial-spectral separability assumption, we show the average correlations of Saab coefficients at the outputs of the first, the second and the third PixelHop++ units in Table 1. The first two rows in the table indicate the averaged spatial correlation of a window of size  $5 \times 5$  at the output of the first (Spatial 1) and the second PixelHop++ units (Spatial 2) for a fixed spectral component. The last three rows indicate the averaged spectral correlation at the output of the first (Spectral 1), the second (Spectral 2) and the third (Spectral 3) Pixelhop++ units at the center pixel location. Only outputs of AC filters are used in the computation. We see that spectral correlations are weaker than spatial correlations. This is especially

obvious for the CIFAR-10 dataset. Furthermore, these correlations are weaker as we go into deeper PixelHop++ units.

**Table 1:** Averaged correlations of filtered AC outputs from the first to the third Pixelhop units with respect to the MNIST, Fashion MNIST and CIFAR-10 datasets.

Dataset	MNIST	Fashion MNIST	CIFAR-10
Spatial 1	$0.48 \pm 0.05$	$0.51 \pm 0.03$	$0.53 \pm 0.03$
Spatial 2	$0.22 \pm 0.03$	$0.29 \pm 0.05$	$0.27 \pm 0.06$
Spectral 1	$0.33 \pm 0.07$	$0.12 \pm 0.02$	$0.0156 \pm 0.0005$
Spectral 2	$0.18 \pm 0.02$	$0.13 \pm 0.01$	$0.0188 \pm 0.0004$
Spectral 3	$0.0099 \pm 0.0001$	$0.0082 \pm 0.0001$	$0.0079 \pm 0.0004$

The weak spectral correlation of Saab coefficients allows us to approximately decompose the joint spatial-spectral input tensor of dimension  $5 \times 5 \times K_i$ ,  $i = 1, 2$ , to the  $(i+1)$ th PixelHop++ Unit into  $K_i$  spatial tensors of size  $5 \times 5$  (i.e., one for each spectral component), respectively. Then, instead of performing the traditional Saab transform of high dimension in PixelHop, we apply  $K_i$  channel-wise (c/w) Saab transforms to each of the spatial tensors in PixelHop++.

The traditional Saab transform and the c/w Saab transform are compared in Fig. 2 from the whole image viewpoint. The traditional Saab transform takes an input image of dimension  $S_i \times S_i \times K'_i$  and generates an output image of dimension  $S_{i+1} \times S_{i+1} \times K'_{i+1}$  after the max-pooling operation that pools from a grid of size  $S_i \times S_i$  to a grid of size  $S_{i+1} \times S_{i+1}$ . The c/w Saab transform takes  $K_i$  channel-images of dimension  $S_i \times S_i$  as the input and generates  $K_{i+1}$  output images of dimension  $S_{i+1} \times S_{i+1}$  after max-pooling.

We adopt the same kernel and bias design principle of the Saab transform in the design of the c/w Saab transform. Their main difference lies in the input tensor size. The dimension of input tensors for PixelHop++ is the spatial neighborhood size ( $5 \times 5 = 25$  in the current example) while that for PixelHop is the multiplication of the spectral dimension and the spatial dimension ( $25 \times K'$ ). Separable transforms, in general, facilitates computation and allows a smaller set of kernel parameters.

#### 3.2. Tree-decomposed Feature Representation

In this subsection, we propose a new feature representation method, called the tree-decomposed feature representation as illustrated in Fig. 3. The root node of the tree is the input image of dimension  $32 \times 32 \times K_0$ , where  $K_0 = 1$  and 3 for the gray-scale and color images, respectively. We normalize the total energy of the root node

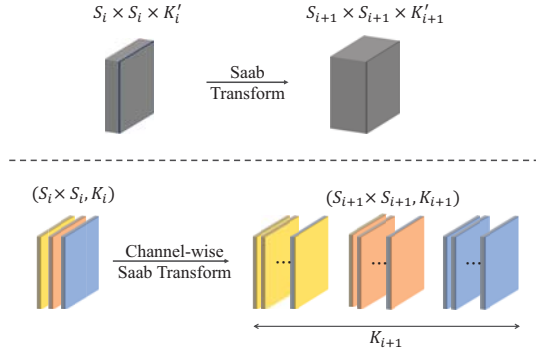


**Fig. 2:** Comparison of the traditional Saab transform and the proposed c/w Saab transform.

to unity. The first PixelHop++ unit yields the first level child nodes. This unit applies the c/w Saab transform of  $5 \times 5$  transform kernels to input images with stride equal to one. Its output contains multiple response maps of dimension  $28 \times 28$ , where the boundary effect is taken into account. We apply the standard  $(2 \times 2)$ -to- $(1 \times 1)$  max-pooling to reduce the spatial redundancy of the response maps. The final output of first PixelHop++ unit is a set of  $K_1$  response maps of dimension  $14 \times 14$ . Each response map is a child node of the root node. The energy of a child node is the multiplication of its parent node energy and its normalized energy with respect to its parent node. **If the energy of a child node is smaller than the pre-set threshold  $T$ , we treat it as a leaf node and the total energy of the response map is used as the feature of the node.** If the energy of a child node is larger than threshold  $T$ , its response map will be used as the input to the next stage for further processing. It is called an intermediate node. For example, there are  $K_i$  nodes at the output of the  $i$ th PixelHop++ unit,  $i = 1, 2$ . We use  $K_{i,1}$  and  $K_{i,2}$  to denote the number of leaf and intermediate nodes at the  $i$ th level in Fig. 1. Clearly,  $K_{i,1} + K_{i,2} = K_i$ .

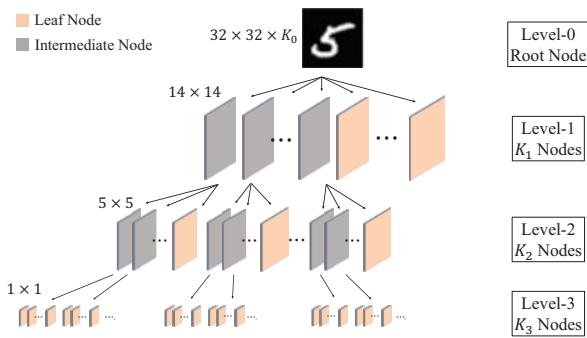


**Fig. 3:** Illustration of the tree-decomposed feature representation.

We conduct the same operation in each PixelHop++ unit successively until the last stage is met. Then, we obtain a tree-decomposed feature representation as shown in Fig. 3, whose leaf node has an associated feature that corresponds to the energy of the response map of one spectral component. The spectral components at different tree

levels have different receptive field sizes. The associated features are useful for the image classification task.

### 3.3. Cross-Entropy-Guided Feature Selection

The tree-decomposed feature representation process is unsupervised. It provides task-independent features. Next, we need to find a link from features to desired labels. In this subsection, we will develop new Module 2 in Fig. 1 based on this representation. First, we compute the cross-entropy value for each feature at the leaf node via

$$L = \sum_{j=1}^J L_j, \quad L_j = - \sum_{c=1}^M y_{j,c} \log(p_{j,c}), \quad (1)$$

where  $M$  is the class number,  $y_{j,c}$  is binary indicator to show whether sample  $j$  is correctly classified, and  $p_{j,c}$  is the probability that sample  $j$  belongs to class  $c$ . The lower the cross-entropy, the higher the discriminant power. We order features from the smallest to the largest cross-entropy scores and select the top  $N_S$  features. This new cross-entropy-guided feature selection process can reduce the model size of the label-assisted regression (LAG) unit.

Finally, we concatenate  $M$  features from each PixelHop++ unit to form a feature vector and fed it into a classifier in Module 3, where a simple linear least-squared regressor is adopted in our experiment. There are two hyperparameters,  $T$  and  $N_S$ , which can be used to control the model size flexibly. We will study their impacts on classification accuracy in Sec. 4.2.

## 4. EXPERIMENTS

### 4.1. Experimental Setup

We test the PixelHop++ method on three popular datasets: MNIST [21], Fashion MNIST [22] and CIFAR-10 [23]. MNIST and Fashion MNIST contain gray-scale images of size  $28 \times 28$  and zero-padding is used to enlarge the image size to  $32 \times 32$ . CIFAR-10 has 10 object classes of color images of size  $32 \times 32$ . We conduct performance benchmarking of PixelHop++ and LeNet-5 [21] in terms of classification accuracy and model complexity. We adopt the original LeNet-5 architecture for MNIST. To handle more complicated images in Fashion MNIST and CIFAR-10, we increase the filter numbers of the convolutional layers and fully-connected layers as shown in Table 2. By applying PixelHop++ to MNIST, we adopt the tree-decomposed feature representation and use features of leaf nodes from the third level only since the discriminant power of features in the first two levels is very weak. For Fashion MNIST and CIFAR-10, we use concatenated features from leaf nodes at all three levels. We set the output dimension,  $M$ , of the LAG unit to  $M = 10$ .

**Table 2:** Comparison of the original and the modified LeNet-5 architectures on three benchmark dataset.

Dataset	MNIST	Fashion MNIST	CIFAR-10
1st Conv. Kernel Size	$5 \times 5 \times 1$	$5 \times 5 \times 1$	$5 \times 5 \times 3$
1st Conv. Kernel No.	6	16	32
2nd Conv. Kernel Size	$5 \times 5 \times 6$	$5 \times 5 \times 16$	$5 \times 5 \times 32$
2nd Conv. Kernel No.	16	32	64
1st FC. Filter No.	120	200	200
2nd FC. Filter No.	84	100	100
Output Node No.	10	10	10

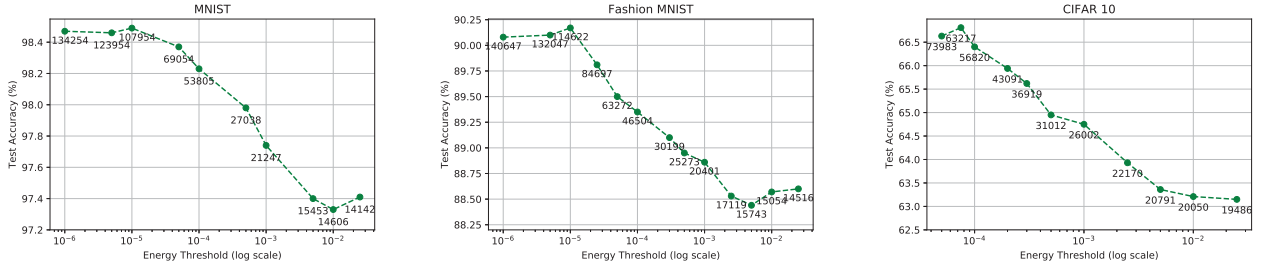


**Fig. 4:** The relation between the test accuracy (%) and energy threshold  $T$  in PixelHop++ for MNIST, Fashion MNIST and CIFAR-10, where the number of model parameters in Module 1 is shown at each operational point.

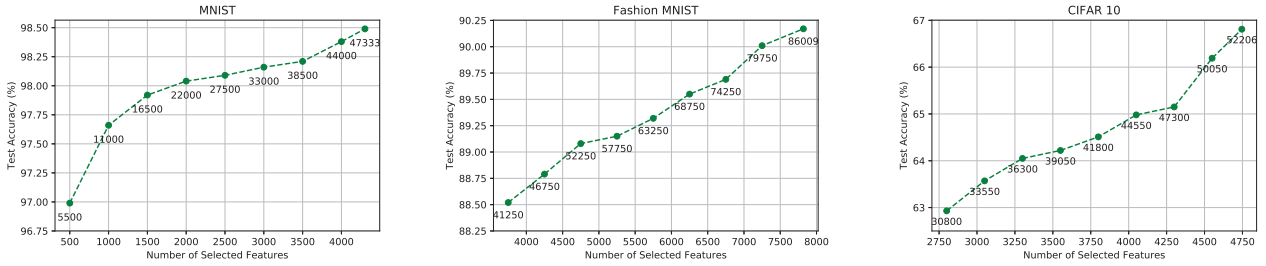


**Fig. 5:** The relation between test accuracy (%) and selected number  $N_S$  of cross-entropy-guided features in PixelHop++ for MNIST, Fashion MNIST and CIFAR-10, where the number of model parameters in Module 2 is shown at each operational point.

#### 4.2. Effects of Hyper-Parameters in PixelHop++

We study the effect of two hyperparameters,  $T$  and  $N_S$ , on classification accuracy of PixelHop++. We can control the model size in Module 1 by energy threshold  $T$ . A larger threshold demands a larger model size. As shown in Fig. 4, the test accuracy decreases slightly as  $T$  decreases while the model size is reduced significantly for all three datasets. For example, by moving  $T$  from 0.00001 and 0.0005 for MNIST, the test accuracy is decreased by 0.51% while the model parameter number becomes 4x fewer. We see clear advantages of the tree-decomposed feature representation in finding good tradeoff.

By varying the  $N_S$  values in Module 2, we plot the test accuracy as a function of  $N_S$  in Fig. 5. The test accuracy decreases marginally as we decrease  $N_S$  to yield smaller models for all three datasets. Take MNIST as an example, the test accuracy of keeping 500 features is only 0.57% lower than keeping all features (3x more) in Module 2. This is because a smaller feature subset with more discriminant features can be selected through the cross-entropy-guided feature selection process. Overall, by adjusting  $T$  and  $N_S$ , we can control the model size in fine-granularity.

#### 4.3. Performance Benchmarking

We compare classification accuracy and model complexity of LeNet-5 and PixelHop++ against all three datasets in Table 3 and Table 4, respectively. Here, we report the performance of two model settings of PixelHop++, *i.e.* a larger model and a smaller model. In terms of classification accuracy, LeNet-5 performs the best on MNIST and CIFAR-10, yet the large PixelHop++ model outperforms LeNet-5 on Fashion MNIST with fewer parameters. On the other hand, by slightly sacrificing the accuracy, PixelHop++ with the small model demands about 2x, 6x and 6x fewer parameters than LeNet-5 for

MNIST, Fashion MNIST and CIFAR-10, respectively. With these performance numbers, we can claim that PixelHop++ is more effective than LeNet-5.

**Table 3:** Comparison of test accuracy (%) of LeNet-5 and PixelHop++ for MNIST, Fashion MNIST and CIFAR-10.

Method	MNIST	Fashion MNIST	CIFAR-10
LeNet-5	99.04	89.74	68.72
PixelHop++ (Large)	98.49	90.17	66.81
PixelHop++ (Small)	97.98	88.84	64.75

**Table 4:** Comparison of the model size (in terms of the total parameter numbers) of LeNet-5 and PixelHop++ for the MNIST, the Fashion MNIST and the CIFAR-10 datasets.

Method	MNIST	Fashion MNIST	CIFAR-10
LeNet-5	61,706	194,558	395,006
PixelHop++ (Large)	111,981	127,186	115,623
PixelHop++ (Small)	29,514	33,017	62,150

## 5. CONCLUSION

An image classification method with a design of interpretable and small learning models was proposed in this paper. Extensive experiments were conducted on three benchmark datasets (MNIST, Fashion MNIST, and CIFAR-10) to demonstrate that the model size of PixelHop++ can be flexibly controlled, and PixelHop++ maintain the classification accuracy with fewer parameters comparing with LeNet-5.



## 6. REFERENCES

- [1] Yu Cheng, Duo Wang, Pan Zhou, and Tao Zhang, "Model compression and acceleration for deep neural networks: The principles, progress, and challenges," *IEEE Signal Processing Magazine*, vol. 35, no. 1, pp. 126–136, 2018.
- [2] Jonathan Frankle and Michael Carbin, "The lottery ticket hypothesis: Finding sparse, trainable neural networks," *arXiv preprint arXiv:1803.03635*, 2018.
- [3] Song Han, Huizi Mao, and William J Dally, "Deep compression: Compressing deep neural networks with pruning, trained quantization and huffman coding," *arXiv preprint arXiv:1510.00149*, 2015.
- [4] Itay Hubara, Matthieu Courbariaux, Daniel Soudry, Ran El-Yaniv, and Yoshua Bengio, "Binarized neural networks," in *Advances in neural information processing systems*, 2016, pp. 4107–4115.
- [5] Mohammad Rastegari, Vicente Ordonez, Joseph Redmon, and Ali Farhadi, "Xnor-net: Imagenet classification using binary convolutional neural networks," in *European conference on computer vision*. Springer, 2016, pp. 525–542.
- [6] Forrest N Iandola, Song Han, Matthew W Moskewicz, Khalid Ashraf, William J Dally, and Kurt Keutzer, "Squeezenet: Alexnet-level accuracy with 50x fewer parameters and 0.5 mb model size," *arXiv preprint arXiv:1602.07360*, 2016.
- [7] Mohammad Javad Shafiee, Francis Li, Brendan Chwyl, and Alexander Wong, "Squishednets: Squishing squeezenet further for edge device scenarios via deep evolutionary synthesis," *arXiv preprint arXiv:1711.07459*, 2017.
- [8] Aline Gondim Santos, Camila Oliveira de Souza, Cleber Zanchettin, David Macedo, Adriano LI Oliveira, and Teresa Ludermit, "Reducing squeezenet storage size with depthwise separable convolutions," in *2018 International Joint Conference on Neural Networks (IJCNN)*. IEEE, 2018, pp. 1–6.
- [9] Yueru Chen and C-C Jay Kuo, "Pixelhop: A successive subspace learning (ssl) method for object recognition," *Journal of Visual Communication and Image Representation*, p. 102749, 2020.
- [10] Min Zhang, Haoxuan You, Pranav Kadam, Shan Liu, and C-C Jay Kuo, "Pointhop: An explainable machine learning method for point cloud classification," *arXiv preprint arXiv:1907.12766*, 2019.
- [11] Matthew Turk and Alex Pentland, "Eigenfaces for recognition," *Journal of cognitive neuroscience*, vol. 3, no. 1, pp. 71–86, 1991.
- [12] Thierry Bouwmans, "Subspace learning for background modeling: A survey," *Recent Patents on Computer Science*, vol. 2, no. 3, pp. 223–234, 2009.
- [13] Hans-Peter Kriegel, Peer Kröger, and Arthur Zimek, "Clustering high-dimensional data: A survey on subspace clustering, pattern-based clustering, and correlation clustering," *ACM Transactions on Knowledge Discovery from Data (TKDD)*, vol. 3, no. 1, pp. 1, 2009.
- [14] Haiping Lu, Konstantinos N Plataniotis, and Anastasios N Venetsanopoulos, "A survey of multilinear subspace learning for tensor data," *Pattern Recognition*, vol. 44, no. 7, pp. 1540–1551, 2011.
- [15] Quanquan Gu, Zhenhui Li, and Jiawei Han, "Joint feature selection and subspace learning," in *Twenty-Second International Joint Conference on Artificial Intelligence*, 2011.
- [16] Kaiye Wang, Ran He, Liang Wang, Wei Wang, and Tieniu Tan, "Joint feature selection and subspace learning for cross-modal retrieval," *IEEE transactions on pattern analysis and machine intelligence*, vol. 38, no. 10, pp. 2010–2023, 2015.
- [17] C.-C. Jay Kuo, "The CNN as a guided multilayer RECOs transform [lecture notes]," *IEEE Signal Processing Magazine*, vol. 34, no. 3, pp. 81–89, 2017.
- [18] C.-C. Jay Kuo and Yueru Chen, "On data-driven Saak transform," *Journal of Visual Communication and Image Representation*, vol. 50, pp. 237–246, 2018.
- [19] C.-C. Jay Kuo, "Understanding convolutional neural networks with a mathematical model," *Journal of Visual Communication and Image Representation*, vol. 41, pp. 406–413, 2016.
- [20] C-C Jay Kuo, Min Zhang, Siyang Li, Jiali Duan, and Yueru Chen, "Interpretable convolutional neural networks via feed-forward design," *Journal of Visual Communication and Image Representation*, vol. 60, pp. 346–359, 2019.
- [21] Yann Lecun, Léon Bottou, Yoshua Bengio, and Patrick Haffner, "Gradient-based learning applied to document recognition," in *Proceedings of the IEEE*, 1998, pp. 2278–2324.
- [22] Han Xiao, Kashif Rasul, and Roland Vollgraf, "Fashion-mnist: a novel image dataset for benchmarking machine learning algorithms," *arXiv preprint arXiv:1708.07747*, 2017.
- [23] Alex Krizhevsky and Geoffrey Hinton, "Learning multiple layers of features from tiny images," Tech. Rep., Citeseer, 2009.